Boron diffusion in MgO and emergence of magnetic ground states: A first-principles study

Hirak Kumar Chandra and Priya Mahadevan
Department of Condensed Matter Physics and Material Sciences, S. N. Bose National Centre for Basic Sciences, Block JD, Sector III, Saltlake, Kolkata 700098, India

(Received 8 May 2013; revised manuscript received 26 February 2014; published 14 April 2014)

It has been reported that in a CoFeB/MgO/CoFeB based tunnel junction, B diffuses into the MgO layer. In this work we consider three possible locations of B in the MgO lattice upon diffusing into the MgO crystal: B substitutes for an Mg site, it substitutes for an O site, or it occupies an interstitial position. Apart from the possibility of introducing midgap states, various charge states of the defect could sustain a local magnetic moment. This could additionally modify the tunnel magneto-resistance ratio. We investigate the electronic structure, the local moment formation, and the formation energies of various defect states. While midgap states are introduced in all three cases, the low formation energy defects are found to be nonmagnetic.

DOI: 10.1103/PhysRevB.89.144412 PACS number(s): 71.55.−i, 71.20.−b, 75.50.Pp

I. INTRODUCTION

Over the last decade we have seen a lot of attention on magnetic tunnel junctions with technological considerations driving the search. Magnetic tunnel junctions are based on the concept of electronic transport between two magnetic layers separated by an insulating barrier region. As the concept of device operation is based on spin-dependent tunneling, a magnetic field can be used to change the direction of the spin orientation in the metal layers, therefore leading to two states—one where the spins are parallel and the resistance is small and the other where the spins are antiparallel and the resistance is large. This switching property allows for applications in many electronic storage devices such as magnetic random access memory [1–3], nonvolatile memory, etc.

The possibility of using magnetic tunnel junction based devices received a strong boost when theoretical calculations using MgO for the insulating barrier and Fe for the electrodes found a tunnel magneto-resistance (TMR) of 1000% [4]. This value has not been achieved experimentally and this has been attributed to interfacial roughness [5,6], barrier thickness [7–9], metal oxidation [10], oxygen vacancies [11], etc. Recently CoFeB [12–17] was put forward as a system which can overcome the problems encountered earlier using Fe as an electrode. B was found to be pushed out of the CoFeB layer but the experimental reports were not clear about where the B atoms went. There have been suggestions of B diffusing into the MgO layer [18–20], forming composites with MgO such as kotoite [20,21], etc. With the recent search for magnetism in dilute magnetic semiconductors, it has been found that certain nonmagnetic impurities when doped into the semiconductors render them magnetic. This has been observed largely when the dopant atoms belong to the first row elements of the periodic table, and the belief has been that it is a Stoner-type mechanism at play [22]. The first row elements introduce localized states in the host semiconductor, which gain energy by intra-atomic Hund's exchange if they can sustain a local moment. This effect is also seen in instances when the doped atoms belong to later rows of the periodic table when they occupy interstitial sites. As these are nonlattice sites their interaction with the host semiconductor is small and so they tend to be more localized and can sustain a magnetic moment. However when they replace lattice sites, they tend to be more delocalized and hence do not sustain a magnetic moment. In the context of TMR materials, this turns out to be an important issue as the diffusion of B from the electrode layer into the insulating barrier region can introduce midgap states which could also be spin polarized. These states could therefore play a role in modifying barrier heights and therefore the TMR ratio. Some aspects of the role of boron in MgO have been examined before. Han *et al.* [23] have concluded from their study that B does not introduce any midgap states, though the only case they considered was B replacing an Mg site. B being a small atom could occupy an interstitial site as well as it could behave as a cation or anion, replacing either Mg or O. Liu *et al.* [24] have considered the case of various group III, IV, and V element dopants replacing O in MgO. The system is found to exhibit half metallic ferromagnetism at the dopant concentrations considered which is found to be 25%. However the case of the metal atom substituting Mg in MgO was found to lead to paramagnetic solutions. In this work we start with the dilute doping limit, typically 3.125%, and examine the consequences of B at various lattice locations in the MgO lattice. While B favors a 3+ charge state, one wonders if B replacing Mg^{2+} or an O^{2-} ion would result in the formation of magnetic centers. This would again modify the TMR ratio.

II. METHODOLOGY

We have used a $2 \times 2 \times 2$ (64 atoms) supercell of MgO with NaCl structure. Three types of configurations have been considered: (1) B replaces an Mg atom, (2) B atom replaces an O atom, and (3) B atom occupies an interstitial position. First-principle calculations based on density functional theory implemented in the Vienna Ab-Initio Simulation Package (VASP) [25] have been carried out to get the total energy of the spin-polarized configurations as well as of the non-spin-polarized configurations. Projector augmented wave [26] potentials with a generalized gradient approximation (GGA) [27] form of the exchange-correlation functional have been used to solve the electronic structure for each of the cases. A γ centered k-point mesh of $4 \times 4 \times 4$ points has been used here. The lattice constant of MgO has been kept fixed at the experimental value of 4.21 Å [28] while the atomic positions have been relaxed till the force on an individual atom was less

 ©2014 American Physical Society

than 0.01 eV/Å. The density of states has been calculated for each of the three cases considering spheres of radii 1 Å around each atom. A cutoff energy of 400 eV has been used for the plane wave basis in the calculations.

Of the three types of defects which we have considered here, we have asked the following question: which defect would be the most likely one to form? This has been examined by calculating the formation energy of each defect. The formation energy of a defect comprising of α atoms with a charge q on the defect is given by [29]

$$\Delta H_f^{\beta,q}(\epsilon_F,\mu) = E(\beta) - E(0) + \sum_\alpha n_\alpha \mu_\alpha^a + q(E_v + \epsilon_F), \quad (1)$$

where $E(\beta)$ and $E(0)$ are the total energies of a supercell with and without the defect β, respectively. This defect β could be a composite defect made up of α atoms. n_α denotes the number of atoms of type α transferred in or out of the host crystal. $n_\alpha = 1$ for an atom removed and $n_\alpha = -1$ for an atom added to the host crystal. μ_α^a denotes their absolute chemical potentials, and q denotes the charge state of the defect. E_v is the energy eigenvalue of the valence band maximum (VBM) at the Γ point of the pure host, and ϵ_F is the Fermi energy which is varied inside the band gap. The energy corresponding to the defect supercell VBM has been corrected by aligning the electrostatic potential on an atom far away from the defect with that calculated in the host. The absolute chemical potential of the elements are estimated as the sum of the energy of the element in its most stable structure, μ_α^s, and an additional energy, μ_α, i.e., $\mu_\alpha^a = \mu_\alpha^s + \mu_\alpha$. For no precipitation of the individual elements one has to take the limits $\mu_{\rm Mg} \leqslant 0$, $\mu_O \leqslant 0$, and $\mu_B \leqslant 0$. In addition the range of values of $\mu_{\rm Mg}$, μ_O, and μ_B are restricted by the constraint that MgO and B_2O_3 do not precipitate out. The calculated values of the formation energies are found to be -6.021 eV for MgO and -15.384 eV for B_2O_3. Hence when we say oxygen-rich conditions, the values of the chemical potentials are $\mu_O = 0$ and $\mu_{\rm Mg} = -6.021$ eV, while when we say Mg-rich conditions, the values of the chemical potential potentials are $\mu_{\rm Mg} = 0$ and $\mu_O = -6.021$ eV. O-rich conditions are typically used at the time of growth of the MgO films.

III. RESULTS AND DISCUSSIONS

MgO occurs in the rock salt structure. The density of states for the host material has been well studied in the literature [30] and we include a brief discussion here for the sake of continuity. The valence band consists primarily of O p states with a width of 4 eV, while the conduction band consists of Mg s states. The experimental band gap is 7.8 eV [31], though as is typical in GGA based calculations, the band gap is found to be 5.5 eV, underestimated from the experimental value.

The choice of B positions in the MgO lattice is determined by the ionic radius of boron as well as its location in the periodic table and we have examined three scenarios. In the first scenario we treated boron as a cation and considered the substitution of an Mg site with B ($B_{\rm Mg}$). In the second scenario we treated B as an anion and considered the case of boron substituting an oxygen atom (B_O). The third scenario that we considered was B occupying an interstitial position, which could happen easily as boron has a small ionic radii associated with it. We have considered each of these cases

TABLE I. Magnetic stabilization energy for various defects when B diffuses into MgO.

Defect type	Magnetic energy (eV)	Nonmagnetic energy (eV)	Magnetic stabilization energy (eV)
$B_{\rm Mg}$	−385.293	−385.172	−0.120
B_O	−378.449	−377.323	−1.127
$B_{\rm int}$	−382.096	−381.998	−0.108

and calculated the formation energy in various charge states as well as examined the electronic and magnetic structure in each case.

Examining the first case of $B_{\rm Mg}$, we initially consider the case where B isovalently substitutes Mg. In this situation B has the same oxidation state as Mg in MgO, i.e., B^{2+}. The electronic configuration of B in such a situation is $2s^1$. As the s levels are partially filled in this case, we calculate the total energy for both the spin-polarized case as well as the non-spin-polarized case to see if a local moment is sustained or not. The magnetic stabilization energy computed as the difference in energy between the spin-polarized calculation and the non-spin-polarized calculation is found to be 120 meV (Table I), indicating that a magnetic solution is favored. Examining the partial density of states (Fig. 1), one finds that the defect-induced levels of s character are found to be totally spin polarized and located within the band gap of MgO. The positions of the VBM as well as the conduction band minimum (CBM) have been determined by considering an oxygen atom as well as an Mg atom far away from the defect. The states on

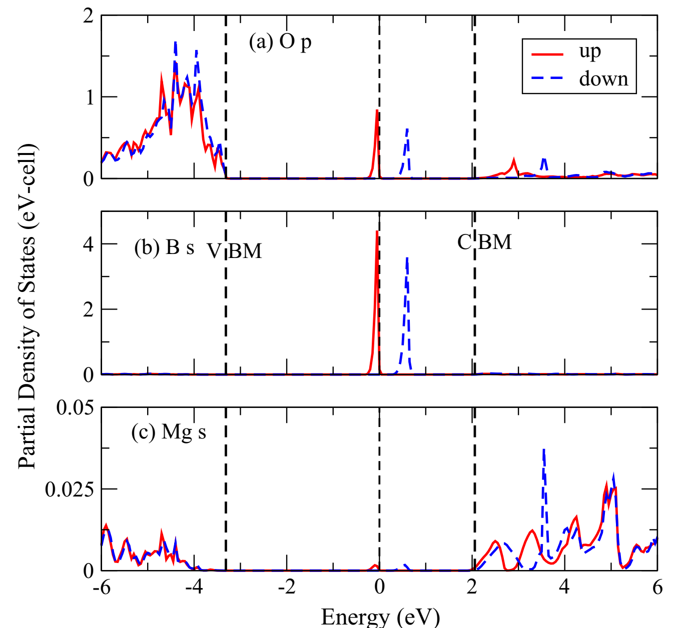

FIG. 1. (Color online) The up (solid line) and down (dashed line) spin partial DOS for (a) O p, (b) B s, and (c) Mg s contributions for the defect $B_{\rm Mg}$ in MgO, where the O and Mg are nearest and second neighbor of the B atom. The VBM and CBM are indicated by the thick dashed lines in the figure. The zero of the energy corresponds to the Fermi energy and is indicated with a dashed vertical line.

these atoms are least likely to be perturbed by the defect. The O p and the Mg s partial density of states are considered to determine the locations of the VBM and the conduction band minimum of the host MgO, which are indicated by dashed lines in Fig. 1. In addition to the B s partial density of states, we have also plotted the O p and Mg s contributions to the partial density of states for an oxygen atom which is the nearest neighbor of the B atom as well as an Mg atom which is the second nearest neighbor of the B atom. One finds significant O p character in the same energy window that one finds the contribution of the B s states, while the contribution from Mg s states is negligibly small. The fact that the impurity states have a significant admixture with the nearest neighbor oxygen p states arises from the fact that the B atom replaces an Mg atom in the lattice. So the picture of the electronic structure before the introduction of the boron could be thought of as consisting of the strongly perturbed states on the nearest neighbor oxygen atoms which lead to dangling bond states in the band gap of MgO. These states interact strongly with the s states on B which is reflected in the partial density of states. Examining the magnetic moments on each atom one finds a moment of 0.38 μ_B on the B atom while one has a moment of 0.06 μ_B on each of the oxygens which are nearest neighbors of the B atom. Adding an electron to the system generates the defect charge state B_{Mg}^{-} which has the $2s$ levels completely filled and hence carries no magnetic moment. The removal of an electron from the system generates the defect with the charge state B_{Mg}^{+} which has the $2s$ levels completely empty and is also nonmagnetic. We examine the formation energies of these configurations later.

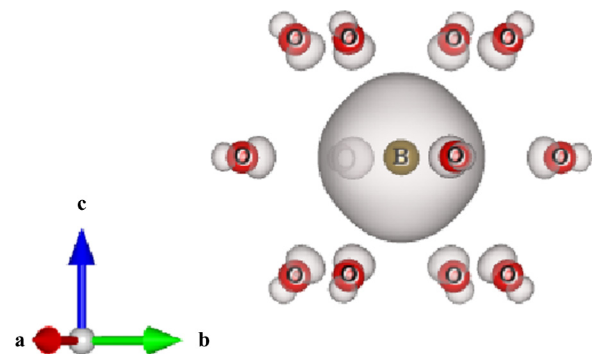

FIG. 3. (Color online) The charge density associated with B_O showing its contributions on B and on oxygen atoms.

The next situation we examined was the case of B substituting an oxygen site in MgO. Assuming an isovalent substitution, the electronic configuration that one expects for B is $2s^2 2p^3$ for a valency of B^{2-}. As this configuration corresponds to a half-filling of the $2p$ states, one finds that the magnetic stability associated with this state is very large and is found to be 1.127 eV as given in Table I. The partial density of states of an oxygen atom which is the second nearest neighbor of the B atom as well as the Mg atom which is the nearest neighbor of the B atom have been plotted in Fig. 2 in addition to the impurity B atom which is now replacing an oxygen atom. As in the earlier cases the energy corresponding

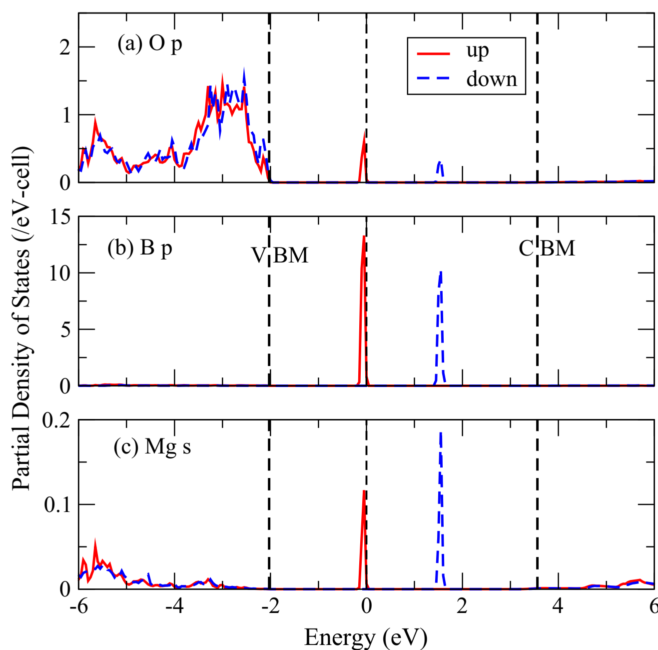

FIG. 2. (Color online) The up (solid line) and down (dashed line) spin partial DOS for (a) O p, (b) B p, and (c) Mg s contributions for the defect B_O in MgO, where the O and Mg atoms correspond to the nearest and second neighbor of the B atom. The VBM and CBM are indicated by the thick dashed lines in the figure. Zero of the energy corresponds to the Fermi energy and is indicated with a dashed vertical line.

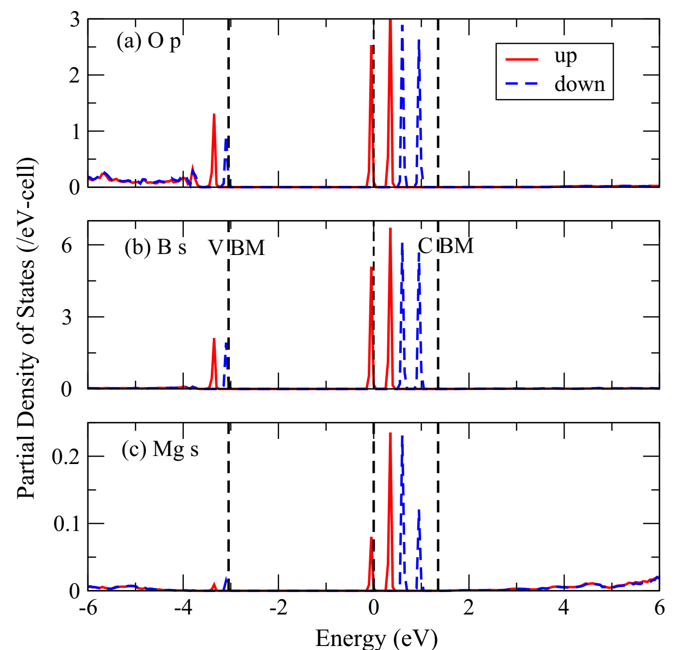

FIG. 4. (Color online) The up (solid line) and down (dashed line) spin partial DOS for (a) O p, (b) B p, and (c) Mg s contributions for the defect B_{int} in MgO, where the O and Mg are the nearest and second neighbor of the B atom. The VBM and CBM are indicated by the thick dashed lines in the figure. Zero of the energy corresponds to the Fermi energy and is indicated with a vertical line.

to the VBM and the CBM of the host material are indicated by the dashed lines. B p states are introduced in the band gap of MgO and the system is found to be insulating. Here the zero of the energy represents the Fermi energy. Unlike in the case of B_{Mg}, we find significant weight of the states on the nearest neighbor Mg atoms as well as the next nearest neighbor O p atoms. The neutral defect B_O has an electronic configuration of $2p^3$ with which one would expect a magnetic moment close to 3 μ_B. However the reduced moment 1.04 μ_B came as a surprise. Plotting the charge density associated with the defect level (Fig. 3) we found it to be very localized within a sphere of larger radii. This is extremely anomalous for a first row element. Considering a larger sphere radius of 2 Å on B for the magnetic moment calculation, we obtain 2.35 μ_B, closer to the expected value. The magnetic moment on the nearest neighbor Mg atom is found to be 0.02 μ_B. The second neighbor O atoms carry a small moment of 0.04 μ_B. Various charge states of B_O are also magnetic. We have also searched for Jahn-Teller distortions in other charge states and find that none are stabilized.

The next kind of defect that we have considered is boron at the interstitial site in MgO. In this case B behaves as an isolated atom and so has the electronic configuration $2s^2 2p^1$ as in elemental B. The magnetic stabilization energy is small, as there is just one electron in the $2p$ levels, and is found to be 108 meV (Table I). The partial densities of states for B_i as well as the Mg atom which is its nearest neighbor and the oxygen atom which is its second neighbor are plotted in Fig. 4. The partial occupancy of B p levels leads to a metallic scenario in the present case. The B p states are mixed with Mg s states of the Mg atom which is its nearest neighbor. Consequently the Mg s states are also spin polarized. Since these states are highly localized, we explored the possibility of Jahn-Teller distortions which may lift the degeneracy. A significantly short bond of 1.28 Å is found between the interstitial B and oxygen. This also drives the system insulating. Examining the magnetic moment on each atom, one finds that the moment on B is found to be 0.3 μ_B while it is found to be 0.13 and 0.03 μ_B on the closest O and Mg atoms, respectively. Here again several charge states of B are found to be magnetic.

Our analysis of the three defects B_{Mg}, B_O, and B_i have shown that several defects could have a magnetic moment associated with them, and these could in turn affect the functioning of the TMR devices. In order to examine which of the studied defects would be most stable, we calculated the formation energies of each of the defects in various charge states as well as under different chemical potentials. The formation energies as a function of Fermi energy are given in Fig. 5. Under Mg-rich conditions one finds that, for small values of ϵ_F, the most stable defect that forms is B_{Mg}^{+1}. This defect is found to be nonmagnetic, as we discussed earlier, as the B $2s$ levels are empty. For intermediate values of the Fermi energy, the defect that is found to be favored is B_O^0. This defect is found to have a large magnetic stabilization energy by virtue of a half-filling of the B $2p$ states. There exists a third regime in which B_O^{-1} defects are found to be stable, and these again can sustain a magnetic moment. While one does find a magnetic moment sustaining defect in these conditions, the formation energies are found to be larger than 10 eV, making them less likely to form.

The type of defects favored under oxygen-rich conditions are, however, different from those found to be favored under Mg-rich conditions. The formation energies are found to be around 5 eV lower than those obtained under Mg-rich

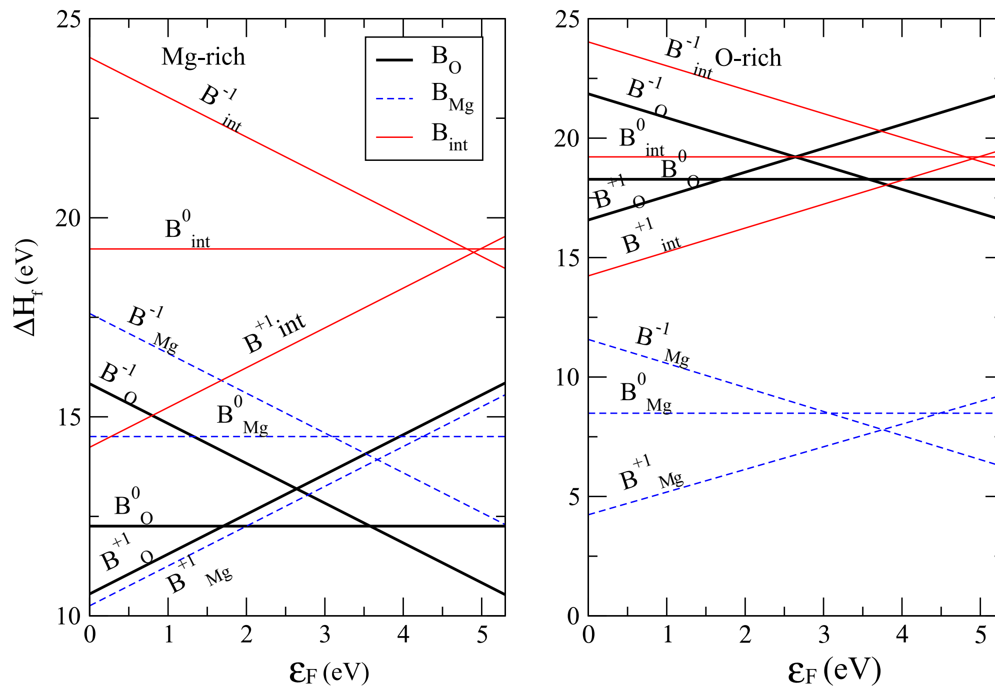

FIG. 5. (Color online) The formation energies of various defects as a function of Fermi energy, ϵ_F, in B-doped MgO have been plotted for (a) Mg-rich and (b) O-rich conditions.

conditions. Both defects in this case leave the system insulating. However neither defect is able to sustain a magnetic moment. So under oxygen-rich conditions one has only nonmagnetic defects introduced by B_{Mg}.

From the density of states calculations, it has been seen that B introduces states within the band gap of MgO. The nonmagnetic defect states are found to be more stable than the magnetic defects from the formation energy calculations. These midgap states reduce the effective band gap of the B-doped MgO compound and hence modify the electron tunneling probability. As a result one can obtain TMR ratios when B diffuses into the MgO layer different than those obtained in the absence of B diffusion.

IV. CONCLUSION

In CoFeB/MgO/CoFeB tunnel junctions, B atoms have been reported to diffuse into the MgO layer. Here we have considered three possible locations of B in the MgO lattice upon diffusing into the MgO crystal. Some of these configurations have been found to be spin polarized and these may change the TMR ratio. The stability of these defect states have been examined by estimating the formation energies of each type of defect for O-rich and Mg-rich conditions. We find that the nonmagnetic defects have the lowest formation energy. However these defects introduce midgap states, the reduction in the band gap would modify the TMR ratio.

[1] M. Hosomi, H. Yamagishi, T. Yamamoto, K. Bessho, Y. Higo, K. Yamane, H. Yamada, M. Shoji, H. Hachino, C. Fukumoto, H. Nagao, and H. Kano, in *IEEE International Conference on Electron Devices Meeting, 2005, IEDM, Technical Digest, 5 December 2005, Washington, DC* (IEEE, Piscataway, NJ, 2005), pp. 459–462.

[2] Z. Diao, D. Apalkov, M. Pakala, Y. Ding, A. Panchula, and Y. Huai, Appl. Phys. Lett. **87**, 232502 (2005).

[3] T. Kawahara, R. Takemura, K. Miura, J. Hayakawa, S. Ikeda, Y. M. Lee, R. Sasaki, Y. Goto, K. Ito, T. Meguro, F. Matsukura, H. Takahashi, H. Matsuoka, and H. Ohno, IEEE J. Solid-State Circuits **43**, 109 (2008).

[4] J. Mathon and A. Umerski, Phys. Rev. B **63**, 220403(R) (2001).

[5] G. I. R. Anderson, H.-X. Wei, N. A. Porter, V. Harnchana, A. P. Brown, R. M. D. Brydson, D. A. Arena, J. Dvorak, X.-F. Han, and C. H. Marrows, J. Appl. Phys. **105**, 063904 (2009).

[6] C. Y. You, T. Ohkubo, Y. K. Takahashi, and K. Hono, J. Appl. Phys. **104**, 033517 (2008).

[7] J. S. Moodera, J. Nowak, L. R. Kinder, P. M. Tedrow, R. J .M. van de Veerdonk, B. A. Smits, M. van Kampen, H. J. M. Swagten, and W. J. M. de Jonge, Phys. Rev. Lett. **83**, 3029 (1999).

[8] S. Yuasa, T. Nagahama, A. Fukushima, Y. Suzuki, and K. Ando, Nat. Mater. **3**, 868 (2004).

[9] W. H. Butler, X.-G. Zhang, T. C. Schulthess, and J. M. MacLaren, Phys. Rev. B **63**, 054416 (2001).

[10] P. Seneor, A. Fert, J.-L. Maurice, F. Montaigne, F. Petroff, and A. Vaures, Appl. Phys. Lett. **74**, 4017 (1999).

[11] G. X. Miao, Y. J. Park, J. S. Moodera, M. Seibt, G. Eilers, and M. Munzenberg, Phys. Rev. Lett. **100**, 246803 (2008).

[12] S. Ikeda, J. Hayakawa, Y. Ashizawa, Y. M. Lee, K. Miura, H. Hasegawa, M. Tsunoda, F. Matsukura, and H. Ohno, Appl. Phys. Lett. **93**, 082508 (2008).

[13] X. Kou, W. Wang, X. Fan, L. R. Shah, R. Tao, and J. Q. Xiao, J. Appl. Phys. **108**, 083901 (2010).

[14] M. Vadala, K. Zhernenkov, M. Wolff, B. P. Toperverg, K. Westerholt, H. Zabel, P. Wisniowski, S. Cardoso, and P. P. Freitas, J. Appl. Phys. **105**, 113911 (2009).

[15] S. Ikeda, K. Miura, H. Yamamoto, K. Mizunuma, H. D. Gan, M. Endo, S. Kanai, J. Hayakawa, F. Matsukura, and H. Ohno, Nat. Mater. **9**, 721 (2010).

[16] M. Kodzuka, T. Ohkubo, K. Hono, S. Ikeda, H. D. Gan, and H. Ohno, J. Appl. Phys. **111**, 043913 (2012).

[17] Y. M. Lee, J. Hayakawa, S. Ikeda, F. Matsukura, and H. Ohno, Appl. Phys. Lett. **90**, 212507 (2007).

[18] Y. Lu, M. Tran, H. Jaffres, P. Seneor, C. Deranlot, F. Petroff, J.-M. George, B. Lepine, S. Ababou, and G. Jezequel, Phys. Rev. Lett. **102**, 176801 (2009).

[19] J. T. Shaw, H. W. Tseng, S. Rajwade, L.-T. Tung, R. A. Buhrman, and E. C. Kan, J. Appl. Phys. **111**, 093908 (2012).

[20] J. J. Cha, J. C. Read, R. A. Buhrman, and D. A. Muller, Appl. Phys. Lett. **91**, 062516 (2007).

[21] D. A. Stewart, Nano Lett. **10**, 263 (2010).

[22] T. Chanier, I. Opahle, M. Sargolzaei, R. Hayn, and M. Lannoo, Phys. Rev. Lett. **100**, 026405 (2008); H. Peng, H. J. Xiang, S.-H. Wei, S.-S. Li, J.-B. Xia, and J. Li, *ibid.* **102**, 017201 (2009); H. K. Chandra and P. Mahadevan, Solid State Commun. **152**, 762 (2012).

[23] Y. Han, J. Han, H. J. Choi, H.-J. Shin, and J. Hong, Appl. Phys. Exp. **5**, 033001 (2012).

[24] G. Liu, S. Ji, L. Yin, G. Fei, and C. Ye, J. Phys.: Condens. Matter **22**, 046002 (2010).

[25] G. Kresse and J. Furthmüller, Phys. Rev. B **54**, 11169 (1996).

[26] G. Kresse and D. Joubert, Phys. Rev. B **59**, 1758 (1999).

[27] J. P. Perdew, K. Burke, and M. Ernzerhof, Phys. Rev. Lett. **77**, 3865 (1996).

[28] International Crystallographic Standard Database.

[29] S. B. Zhang, S. H. Wei, and A. Zunger, Phys. Rev. Lett. **78**, 4059 (1997); S. B. Zhang, S. H. Wei, A. Zunger, and H. Katayama-Yoshida, Phys. Rev. B **57**, 9642 (1998); C. G. Van de Walle, Phys. Rev. Lett. **85**, 1012 (2000); P. Mahadevan and A. Zunger, Phys. Rev. B **68**, 075202 (2003).

[30] S. V. Nistor, E. Goovaerts, and D. Schoemaker, Phys. Rev. B **52**, 12 (1995); T. Bredow and A. R. Gerson, *ibid.* **61**, 5194 (2000).

[31] D. M. Roesler and W. C. Welker, Phys. Rev. **154**, 861 (1967).